A rheometry method to assess the evaporation-induced mechanical strength development of polymer solutions used for membrane applications

Eduard Caicedo-Casso[1], Jessica Sargent[2], Rachel M. Dorin[3,ξ], Ulrich B. Wiesner[3], William A. Phillip[4], Bryan W. Boudouris[2,5], and Kendra A. Erk[1]*

[1] School of Materials Engineering, Purdue University, West Lafayette, IN 47907
[2] Davidson School of Chemical Engineering, Purdue University, West Lafayette, IN 47907
[3] Department of Materials Science and Engineering, Cornell University, Ithaca, NY 14853-1505
[4] Department of Chemical and Biomolecular Engineering, University of Notre Dame, Notre Dame, IN 46556
[5] Department of Chemistry, Purdue University, West Lafayette, IN 47907
[ξ]Current address: TeraPore Technologies, Inc., South San Francisco, CA 94080
*corresponding author: erk@purdue.edu

ABSTRACT

Rotational and oscillatory shear rheometry were used to quantify the flow behavior under minimal and significant solvent evaporation conditions for polymer solutions used to fabricate isoporous asymmetric membranes by the self-assembly and non-solvent induced phase separation (SNIPS) method. Three different A-B-C triblock terpolymer chemistries of similar molar mass were evaluated: polyisoprene-*b*-polystyrene-*b*-poly(4-vinylpyridine) (ISV); polyisoprene-*b*-polystyrene-*b*-poly(*N*,*N*-dimethylacrylamide) (ISD); and polyisoprene-*b*-polystyrene-*b*-poly(*tert*-butyl methacrylate) (ISB). Solvent evaporation resulted in the formation of a viscoelastic film typical of asymmetric membranes. Solution viscosity and film viscoelasticity were strongly dependent on the chemical structure of the triblock terpolymer molecules. A hierarchical magnitude (ISV>ISB>ISD) was observed for both properties, with ISV solutions displaying the greatest solution viscosity, fastest film strength development, and greatest strength magnitude.

1.0 INTRODUCTION

The self-assembly and non-solvent induced phase separation (SNIPS) method is an innovative membrane fabrication technique for block copolymer-based separation devices.[1] [2] [3] [4] The SNIPS method consists of the preparation of a polymer solution, then the casting of the polymer solution into a film, followed by a controlled solvent evaporation step, before a rapid solvent to non-solvent exchange that is used to precipitate the polymer and create the final nanoporous membrane.[5] The result is an asymmetric membrane with a periodically-ordered structure in the top selective/separation layer that offers excellent performance as a filtration device and as a chemically-tailored adsorbent material with high fouling resistance.[6] [7] [8] [9] The high solute selectivity as well as the high solvent permeability are key properties of SNIPS membranes that

are the direct result of the high density of uniform pores obtained by the assembly of block copolymers.[7]

A SNIPS membrane is comprised of a hierarchical tapered structure.[10] The selective layer is the result of block copolymer assembly and exhibits a well-ordered structure with a high density of uniform nanoscale pores, the main function of which is to separate solutes from the solvent.[3] The asymmetric substructure mechanically supports the selective layer, allowing the membrane to withstand the stresses experienced by the film during the process of filtration. This support layer also facilitates a rapid passage of solvent through an asymmetric macro-void structure, which minimizes the fluid drag resistance during practical membrane operation.[11] The necessary components of the SNIPS process are the self-assembled block copolymer, a mixed solvent system to prepare the polymer solution, and a non-solvent bath. The block copolymer and the components of the solvent mixture interact with each other to create the selective layer via self-assembly upon solvent evaporation. Upon phase inversion induced by the non-solvent bath (i.e., polymer-solvent de-mixing), the non-equilibrium structures of selective and support layers precipitate from solution.[12]

Membrane scientists have shown that SNIPS membranes can outperform current commercial materials. [4 9] Recent research focused on membranes created through the combination of self-assembly and phase inversion has concentrated on the interrelationship of the molecular architecture with the final membrane morphology and separation performance.[6] Importantly, however, one of the major challenges towards the creation of a commercial filtration membrane is to manufacture these revolutionary new materials by continuous casting techniques (e.g., a roll-to-roll process).[7] To increase the scale of membrane production, the SNIPS process must be adapted to a scalable manufacturing environment and, specifically, the film translation steps that occur during roll-to-roll casting. This adjustment involves the introduction of new variables such as convection, shear stresses, and film deformation.[13]

Consequently, elucidating the behavior of the block copolymers and the solvent evaporation at early stages is imperative to accurately translate the SNIPS membrane from the laboratory scale to a commercial-scale product. Mechanisms regarding the self-assembly process and final assembled morphology have been proposed by Dorin, *et al.,* [6] Sargent, *et al*., [7] Gu, *et al.,*[14] and Rangou, *et al.* [15] Also, the effect of relative humidity over the final assembled morphology have been elucidated by Li, *et al*.[16] However, the roles of block copolymer chemistry and solvent evaporation over the mechanical evolution of SNIPS membranes are still poorly understood.

Solvent evaporation is a critical step in the creation of a desired membrane morphology. The structural evolution of the selective layer takes place over a short solvent evaporation window. [14] The necessary and allowable evaporation window is different for every polymer-solvent combination and partially defines the success of obtaining a desired morphology during processing. By using an appropriate block chemistry and a selective solvent mixture, polymer self-assembly can lead to a perpendicular-to-surface oriented cylinder structure or a cubic arrangement

of channels useful in filtration applications. [1] [10] The feasibility of obtaining a desired morphology depends on the block copolymer and the selective solvent system as well as the solvent evaporation rate and time.[17] Hypotheses have been proposed in order to correlate the solvent evaporation rate to the orientation of the self-assembled cylinders.[18] [19] Phillip, *et al.*, stated that a relatively fast solvent evaporation rate is necessary to obtain perpendicular-to-surface orientated cylinders. A high solvent evaporation rate will reduce the bulk solvent concentration to a value below a critical concentration; this reduction in solvent concentration leads to the nucleation and continuous growth of oriented cylinders giving rise to the selective layer of a SNIPS membrane.

The continuous growth of the selective layer depends on the ability of the solvent to diffuse through a polymer matrix.[18] [20] However, the viscoelasticity of the sample and the feasibility of preserving a desired morphology over the time (before non-solvent exchange) are influenced by the physicochemical nature of the selective layer. [20]

The viscoelastic behavior is typical of all polymeric materials. [21] The polymers used in SNIPS membrane fabrication are expected to show a rheological viscoelastic behavior similar to those of associative block copolymers. [22] [23] Associative block copolymers assemble in regular and diverse structures creating unique intermolecular interactions (bridges) that are dependent on the physicochemical nature of the block copolymer – solvent system. [22] [24] The amount and life-time of the individual or cumulative bridges defines the viscoelastic behavior of associative polymers. [22] Higher numbers and life-times of the bridges suggest higher viscosities and greater solid-like behavior. Consequently, it is expected that phase separation due to solvent evaporation in a particular polymer system produces a unique intermolecular interaction that can be observed in the evolution of the viscoelastic behavior of SNIPS polymer solutions. The evolution of the viscoelasticity can be seen as the transition from liquid-like to solid-like rheological behavior. [25] Out of all available methods to measure the viscoelastic evolution of a thin film of solution, the most suitable method in this case, where solvent is allowed to evaporate, is dynamic sinusoidal oscillations within a small strain experimental range. The above choice is made because the method preserves the integrity of the sample such that the effects of solvent evaporation can be isolated. [21]

This paper uses shear rheometry measurements to directly quantify the flow behavior and the effect of solvent evaporation over the mechanical strength development of polymer solutions used to produce SNIPS membranes. A relationship between the chemical structure of block copolymers and the viscoelastic response is demonstrated. Rotational shear experiments are used to quantify the flow behavior under shear deformation of most common polymer systems, and oscillatory shear experiments are applied to elucidate the mechanical development of SNIPS solutions upon solvent evaporation.

2.0 EXPERIMENTAL METHODS

2.1 Polymer Synthesis

Polyisoprene-*b*-polystyrene-*b*-poly(4-vinylpyridine) (ISV) was synthesized using sequential anionic polymerization as previously reported by Phillip, *et al.* [17] Polyisoprene-*b*-polystyrene-*b*-poly(*tert*-butyl methacrylate) (ISB) and polyisoprene-*b*-polystyrene-*b*-poly(*N*,*N*-dimethylacrylamide) (ISD) were synthesized using the controlled radical polymerization method of reversible addition-fragmentation chain transfer (RAFT) polymerization.[26] The synthesis of ISD has been previously reported by Mulvenna, *et al.*,[3] but the synthesis of the ISB used in this study has not previously been documented.

ISB was synthesized using a reaction scheme similar to that reported for the synthesis of ISD. All reagents were purified and all polymer products were characterized according to previous literature reports.[3] A brief description of an ISB synthetic procedure is outlined herein. A reaction solution of 15 mL isoprene, 54.7 mg 2-(dodecylthiocarbonothioylthio)-2-methylpropionic acid (CTA), and 5.5 µL *tert*-butyl peroxide was combined in a 25 mL reaction flask (Chemglass) containing a polytetrafluoroethylene-coated (PTFE-coated) magnetic stir bar. The freeze-pump-thaw method was repeated 3 times to evacuate residual air from the reaction mixture, and the reaction flask was refilled with argon. The reaction proceeded by stirring the solution in an oil bath at 120 °C for 22 hours. The solution was cooled to room temperature, precipitated in excess methanol (J.T. Baker), and dried under vacuum for 24 hours ($M_{n(PI)}$ = 9.6 kg mol^{-1}). 1.3 g of dried polyisoprene (PI) was combined with 35.4 mL styrene and 3.3 mg 2,2'-azobis(2-methylpropionitrile) (AIBN) in a reaction vessel containing a PTFE-coated stir bar. The vessel was evacuated and refilled in the same manner as for PI, and the solution was reacted by stirring at 60 °C for 20 hours. The solution was then cooled to room temperature, precipitated in excess methanol, and dried under vacuum for 24 hours ($M_{n(PS)}$ = 18.7 kg mol^{-1}). 2.7 g of dried polyisoprene-*b*-polystyrene (PI-PS) was then combined with 5.1 mL *tert*-butyl methacrylate, 11.7 mL THF, and 2.5 mg AIBN in a reaction vessel containing a PTFE-coated stir bar. The vessel was evacuated and refilled in the same manner as previous reactions, and the solution was reacted by stirring at 60 °C for 3.5 hours. The solution was then cooled to room temperature, precipitated in excess methanol, and dried under vacuum for 24 hours ($M_{n(PtBMA)}$ = 15.7 kg mol^{-1}). The final dispersity of this polymer was 1.5.

Figure 1 presents the chemical structure of all three triblock terpolymer samples utilized in this study. Table 1 reports the physical and chemical characteristics of each sample, showing that all three polymers exhibit similar overall molar mass and dispersity (**Đ**) values.

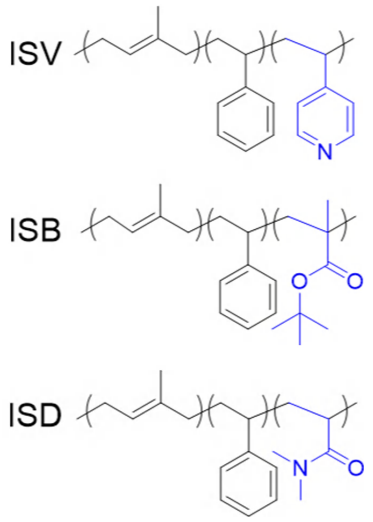

Figure 1. Triblock terpolymer molecular structures for: polyisoprene-*b*-polystyrene-*b*-poly(4-vinylpyridine) (ISV), polyisoprene-*b*-polystyrene-*b*-poly(*tert*-butyl methacrylate) (ISB), and polyisoprene-*b*-polystyrene-*b*-poly(*N*,*N*-dimethylacrylamide) (ISD).

Table 1. Composition of the polymers investigated in this study.

A-B-C Block Polymer	**M_n (kg mol^{-1})**	**Đ**	**Volume Composition (%) of A/B/C Moieties**
ISV [polyisoprene-*b*-polystryrene-*b*-poly(4-vinylpyridine)]	43.0	1.02	27/55/18
ISB [polyisoprene-*b*-polystryrene-*b*-poly(*tert*-butyl methacrylate)]	40.1	1.50	24/41/35
ISD [polyisoprene-*b*-polystryrene-*b*-poly(*N*,*N*-dimethylacrylamide)]	42.3	1.40	21/43/36

2.2 Characterization

2.2.1 Flow Behavior at Constant Concentration

Rotational shear rheometry was used to characterize the flow behavior of ISV, ISB and ISD terpolymer solutions at three different terpolymer concentrations (9 wt.%, 12 wt.% and 15 wt.%). An Anton Paar MCR702 rheometer coupled with a 10 mm Couette fixture and solvent trap were employed to execute all rotational shear experiments in the absence of solvent evaporation. The sample volume used in each experiment was 1.2 ml. In this case the terpolymer concentration was kept constant; therefore, the internal structure of the sample was only subject to changes induced by shear deformation. Logarithmic ramps of shear rate were used to construct the flow profile. Shear rate control and 3 seconds of data averaging were used to reach steady state at each measured point. The temperature was held constant at 22 ºC over all experiments using a Peltier system.

For all rheological studies, solid terpolymer was dissolved using a solvent mixture of 70% 1,4-dioxane (DOX) (Sigma Aldrich) and 30% tetrahydrofuran (THF) (Fisher Scientific), by weight. The polymer solutions were magnetically stirred for 6 hours and allowed to degas overnight before testing.

2.2.2 Mechanical Strength Development upon Solvent Evaporation

The results of the rotational experiments were meaningful because the internal structure of the sample only suffered deformation induced by shear (e.g., rotational shear at a constant polymer concentration). In the case of samples with variable polymer concentration, the results generated from oscillatory experiments are more meaningful. Different than the rotational shear experiments, the oscillatory shear experiments measured the mechanical response of the sample over time to small sinusoidal deformations of a set amplitude and frequency. [25]

Oscillatory shear rheometry was used to evaluate the development of mechanical strength upon solvent evaporation from the ISV, ISB, and ISD terpolymer solutions. The initial concentrations were set (9 wt.%, 12 wt.% and 15 wt.%) and they changed with time due to solvent evaporation. A TA Instruments ARG2 rheometer coupled with 40 mm parallel plates was used to allow solvent evaporation while measuring the apparent storage modulus (*G'*) and apparent loss modulus (*G"*) over time; *G'* and *G"* are reported as apparent properties because the composition of the film is not uniform and varies over the course of the experiment due to solvent evaporation. The gap between plates was 0.4 mm yielding to a sample volume of 0.6 mL. In order to visualize and isolate the solvent evaporation effects, the use of small amplitude oscillatory shear (SAOS) rheometry was imperative. To perform SAOS, it was necessary to determine the linear viscoelastic range (LVR). The amplitude sweep test is traditionally the most appropriate tool to determine the LVR; however, an amplitude test on a sample in which the viscosity changes over time due to solvent evaporation would not be representative for this physical phenomenon. Therefore, a second approach that involved the use of a 15wt. % ISB solution and time sweeps at different strain values (0.1%, 0.5%, 1% and 2% strain) was used. This approach assumes that the viscoelastic material response to sinusoidal strain is linear as long as the applied strain is within the LVR. Hence, an applied strain within the LVR would produce equivalent responses of *G'* and *G"*. Based on the results of this determination test, a strain of 0.5% and an oscillation frequency of 10 rad s^{-1} were used as oscillatory parameters for all subsequent experiments. The temperature was held constant at 22 ^{o}C over all experiments using a Peltier system.

To quantify the development of mechanical strength upon solvent evaporation, four parameters were calculated from the oscillatory data: the initial slope, the plateau slope, the cross-over point, and the average *G'* plateau value.

The initial slope was calculated using a linear regression over *G'* data for $t < 30$ s. This initial increase in slope provides an approximate measure of the formation rate of a viscoelastic film right at the edge of the parallel plates upon initial solvent evaporation. The plateau slope was calculated using a linear regression over *G'* data for $300 \text{ s} < t < 600$ s. The plateau slope can be employed to

determine the rate of elasticity development of the elastic film upon continuous solvent evaporation. The cross-over point was calculated via regression-extrapolation using the phase shift (*i.e., tan δ*) data close to a value of 1. The cross-over point represents the time at which the viscoelastic behavior of the sample changes from a predominantly viscous to an elastic response. The average *G"* plateau was calculated by averaging the *G"* data for t > 300s. The average *G"* plateau is an approximation of the hypothetical value of the maximum elastic strength of a SNIPS-casted film prior to the non-solvent exchange step with the solvent. Note that all four parameters are graphically illustrated in Figure 2.

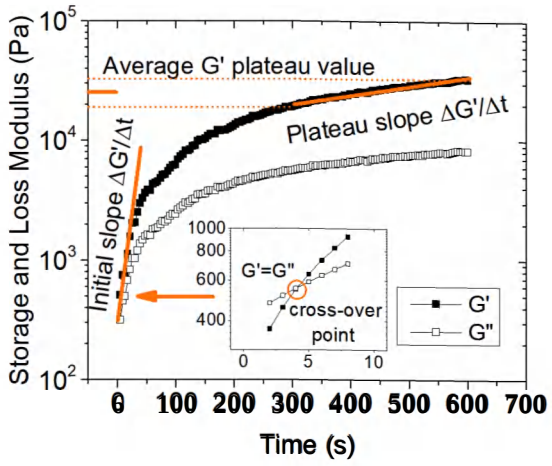

Figure 2. Illustration of the four parameters calculated from the oscillatory test upon solvent evaporation (0.5% strain and 10 rads^{-1} angular frequency).

The change in mass over time of the cast films was quantified to determine the diffusion coefficient of the solvent through the cast polymer film. A film with an enclosed area of 5 cm^2 and a thickness of 382 μm was cast on a glass slide for evaporation. The sample was massed on an Acculab ALC-210.4 scale with a maximum mass measurement of 210 g and accuracy up to 0.0001 g. The change in mass over time data was gathered over a 15-minute time period. The ability of the solvent to evaporate from a cast film was related to the resistance that the solvent encounters to diffuse from the bulk solution to the solution-gas interface with similar analysis previously reported.[18] Hence, the change in mass of a cast film can be related to the solvent diffusivity through a solidifying film using Equation 1.[27,28]

$$\frac{M_0 - M}{A_m} = \sqrt{2Dt}C_b \quad (1)$$

Here the parameters are defined as the instantaneous mass (M), the initial mass (M_0), the evaporation area (A_m), the diffusion coefficient (D), time (t), and the bulk solvent concentration (C_b). Equation 1 is a 1D model considered valid due to the relative thin film compared to the large cross-sectional area (steady state Fickian diffusion).[29] Convection terms are not included in the derivation of Equation 1 because the solvent mass transport in the gas phase is not considered to be the limiting factor for solvent diffusion.[18] The change in mass of a cast film within a specific

evaporation area is compared to the square root of time. As a result, the diffusion coefficient of solvent within a polymer film can be calculated via linear regression methods.

3.0 RESULTS

3.1 Rheometry results with minimal evaporation

Figure 3 shows a schematic of the rotational test set up and viscosity curve results for the ISV, ISB, and ISD solutions at 15 wt.%, under no evaporation effects. The viscosity behavior under rotational shear of all three solutions corresponds to a Newtonian behavior within the range of the studied shear rates. Polymer solutions at concentrations of 9 wt.% and 12 wt.% are also expected to exhibit Newtonian behavior but at reduced viscosities. These results are not reported because the measurements were too close to the minimum torque resolution limit of the Anton Paar rheometer (0.01 μN m).

Despite the Newtonian response, the three solutions exhibited different values of Newtonian viscosity. The ISV (70 $mPas^{-1}$) and ISD (14 $mPas^{-1}$) solutions showed the highest and lowest viscosity, respectively. The ISB solution (22 $mPas^{-1}$) showed an intermediate viscosity.

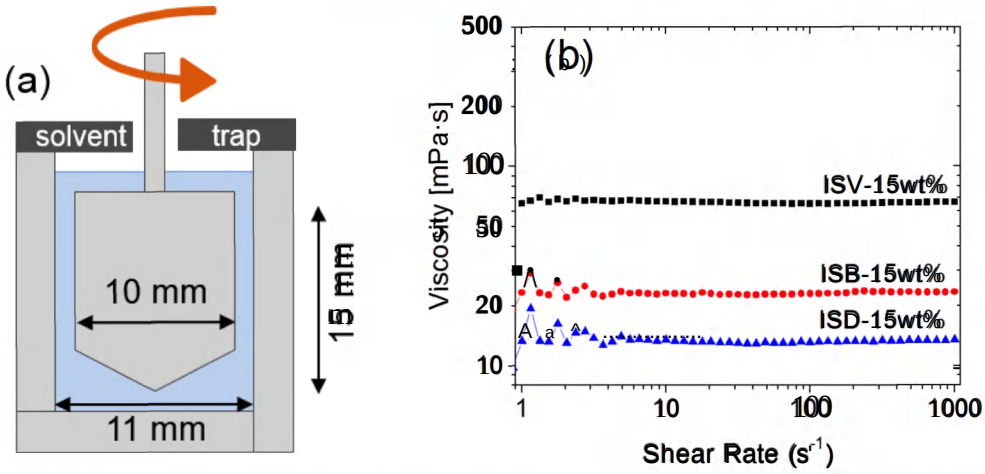

Figure 3. (a) Schematic of the 10-mm Couette fixture with a solvent trap used in rotational rheometry experiments. Solvent evaporation is discouraged by this configuration. (b) Viscosity curves of ISV, ISB, and ISD solutions at 15 wt.% terpolymer concentration using the Couette fixture to avoid solvent evaporation.

3.2 Rheometry results with significant evaporation

Figure 4 shows the results for the LVR determination test used in this experiment. An ISB solution with 15 wt.% initial terpolymer concentration was used. The *G'* response to sinusoidal deformation as a function of time at different values of strain is reported. High strain (2%) produced a lower mechanical strength development compared to low strain (0.1%). Additionally, high strain produced significant noise that suggests a non-linear response to sinusoidal deformation. Figure 4 shows that only strain values of 0.1%, 0.5% and 1% behaved similarly, even after significant solvent evaporation. The above statements suggest that 2% strain is already outside the LVR, and,

0.1%, 0.5% and 1% strain values are close to or within the LVR. Consequently, a 0.5% strain was selected for use in oscillatory experiments as it is within the SAOS regime.

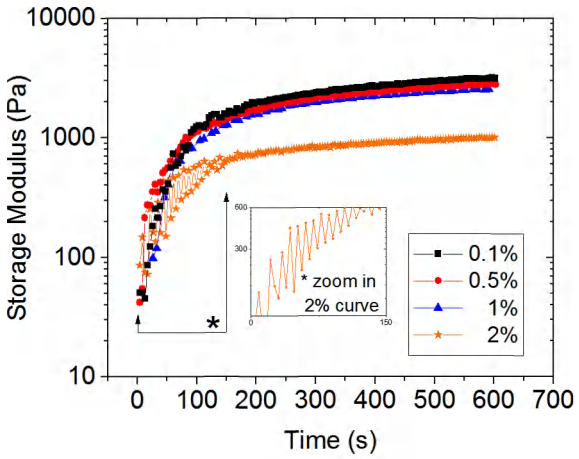

Figure 4. LVR determination: time sweep of a ISB solution at 15 wt.% initial terpolymer concentration. 0.1%, 0.5%, 1% and 2% strain points were evaluated at an oscillatory frequency of 10 rad/s.

During the oscillatory experiments, G' and G'' showed a similar trend in their evolution. As seen in Figure 2, G' and G'' rapidly increase over several orders of magnitude, during the initial seconds of the test. At longer times, both moduli tend to attain a steady state value. G' or G'' predominance is a function of time. In the initial seconds of the experiment, $G'' > G'$, indicating that the sample exhibits a viscous behavior, as expected for the predominantly solvent-containing solutions. Yet, the predominant behavior turns to $G' > G''$ just few seconds after time zero. This suggests that the solvent evaporation produces a transition from viscous to elastic response in each tested sample. This transition is represented by the cross-over point, which is the time when $G'=G''$.

Figure 5 shows the G' and G'' development upon solvent evaporation at different initial terpolymer concentrations for ISV (Figure 5a), ISB (Figure 5b), and ISD (Figure 5c) solutions. The general trend of G' and G'' evolution is similar but differs in extent due to differences in chemistry of the triblock terpolymer and the initial terpolymer concentration. These results are summarized in Figure 6. Figure 6 reports the initial slope, plateau slope and average G' plateau for each sample (as defined in Figure 2). At the same initial terpolymer concentration, the ISV solution exhibits the highest and fastest mechanical strength development represented by the highest average G' plateau and the highest initial slope, respectively. ISB follows at an intermediate magnitude and rate, and ISD displays the lowest magnitude and slowest rate.

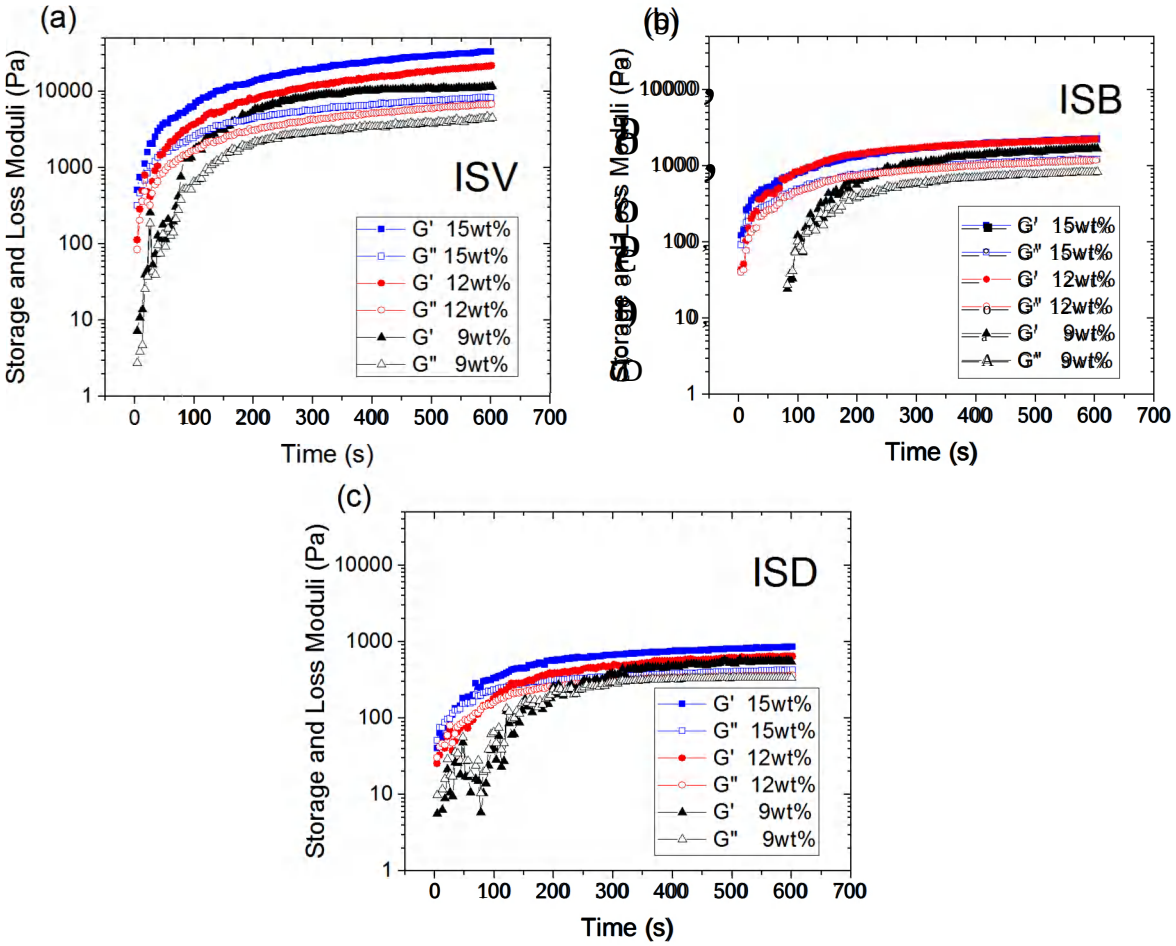

Figure 5. Mechanical strength development upon solvent evaporation; 9 wt.%, 12 wt.%, and 15 wt.% initial terpolymer concentrations for (a) ISV, (b) ISB, and (c) ISD solutions.

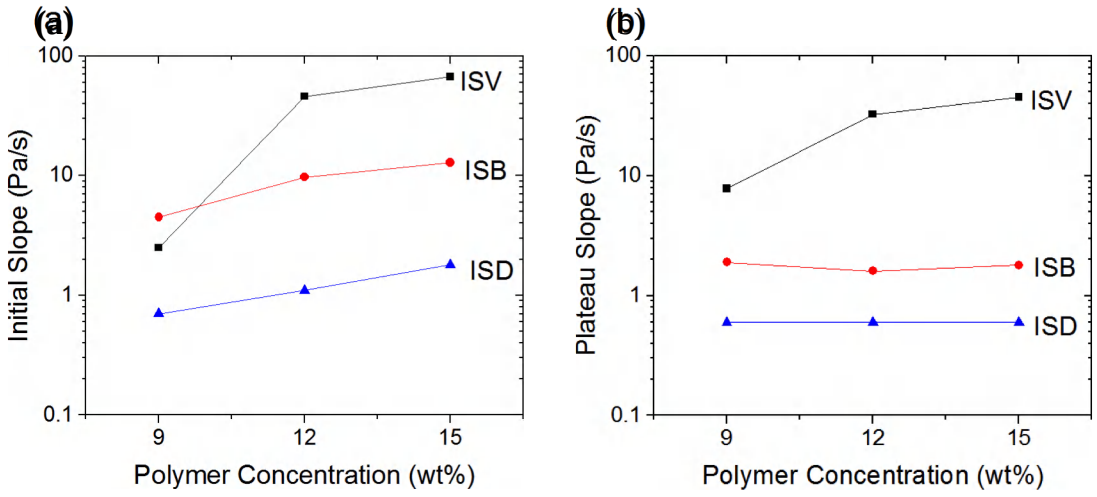

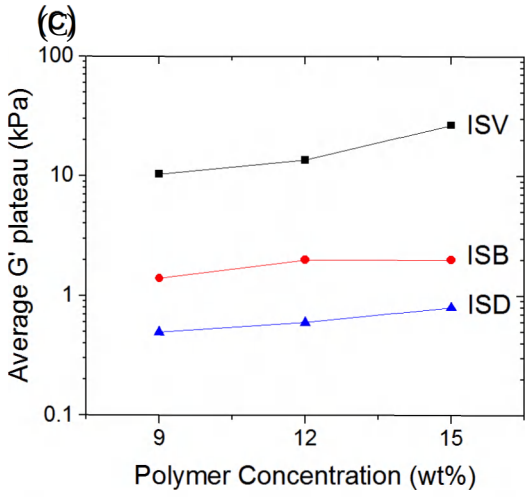

Figure 6. (a) Initial slope, (b) plateau slope, and (c) average *G'* plateau for ISV, ISB, and ISD solutions at 9 wt.%, 12 wt.% and 15 wt.% initial terpolymer concentrations; data calculated from the results in Figure 5.

Considering the same triblock terpolymer material, it is observed that the initial polymer concentration is the factor that drives the rate and extent of the mechanical strength development. The greater the initial polymer concentration, the greater the initial slope and average *G'* plateau shown in Figure 6. On the contrary, the trend with increasing initial polymer concentration is inverted for the cross over point measurement (Figure 7). That is, Figure 7 shows that greater terpolymer concentrations reduce the cross-over point considering the same triblock terpolymer material.

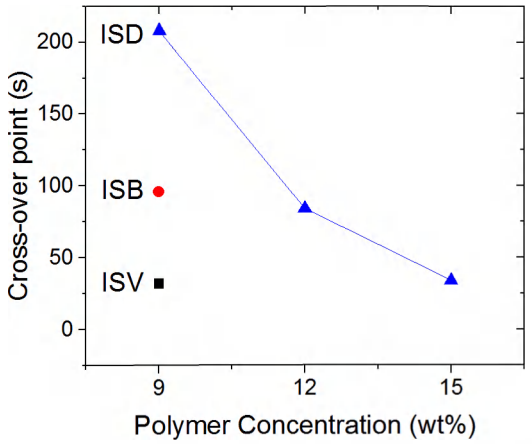

Figure 7. Viscous-to-elastic cross-over points for ISV, ISB, and ISD solutions initially at 9wt.%, 12wt.%, and 15wt.% terpolymer concentrations. These data are calculated from results in Figure 5.

An interesting finding is that the cross-over point data in Figure 7 seems to follow different trends with respect to block chemistry. The ISD solution at 9 wt.% initial concentration shows the latest cross-over point compared to solutions ISV and ISB. It is expected that solutions at 12 wt.% and 15wt % also follow the same trend. ISV and ISB solutions at 9 wt.% initial concentrations show a

cross-over point equal to 32 s and 96 s, respectively. However, cross-over points for ISV and ISB solutions at 12 wt.% and 15 wt.% are not shown because the points occur too quickly to accurately be resolved by the rheometer.

3.3 Solvent evaporation studies

As shown in Figure 8, the apparent diffusion coefficient (D) of the THF-DOX (30-70) solvent mixture in ISV, ISB, and ISD films was independent of solution concentration and triblock terpolymer chemistry. The diffusion coefficient varied from 1.02 x 10^{-6} to 1.31 x 10^{-6} cm^2 s^{-1} for the different chemistries and initial terpolymer concentrations evaluated here, with overlapping standard deviation in average D values. Consequently, any variation in D was not statistically significant, and the solvent diffusion coefficient was considered to be similar for all samples.

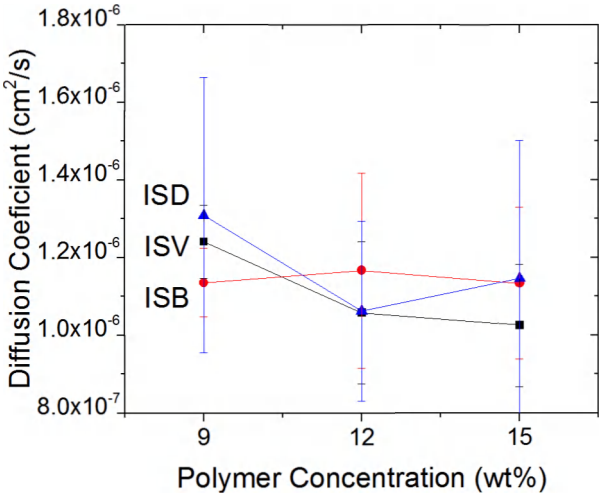

Figure 8. Diffusion coefficient for a solvent mixture of THF-DOX (30-70) through ISV, ISB and ISD terpolymer films. The initial terpolymer concentrations were 9wt.%, 12wt.%, and 15wt.%.

4.0 DISCUSSION

4.1 The effect of block chemistry on the flow behavior (no evaporation)

Rotational rheometry has been employed previously to study SNIPS polymer solutions, with a particular focus on determining the effects of polymer solution concentration through the measurement of solution viscosity.[15] Previous literature stated that block polymers in solution with low viscosities (low polymer concentrations) have a tendency to precipitate asymmetric membranes with finger-like macro-voids. [30, 23] These finger-like domains are desirable as a support layer for SNIPS membranes because they provide a lower resistance to the flow of solvent during filtration and adsorptive applications. Conversely, block polymers in solution with a high viscosity (high polymer concentration) have a tendency to precipitate a sponge-like support structure due to losses in chain mobility. This sponge-like structure is a less-desirable result for membrane performance because its higher resistance to flow results in a lower permeability.[31] Consequently,

the study of the effects of polymer chemistry on the viscosity of the SNIPS polymer solutions may be used to tune the final microstructure of SNIPS membranes.[32]

The viscosity responses (η) displayed in Figure 3b for 15 wt.% ISV, ISB, and ISD solutions are Newtonian (i.e., independent of shear rate), with $\eta_{ISV} > \eta_{ISB} > \eta_{ISD}$. This response is characteristic of a dilute polymer solution, where the intermolecular forces are negligible in comparison to the hydrodynamic forces between the polymer molecules and the solvent.[33 34] Then, the viscosity is directly dependent on the displaced volume of each polymer molecule in solution (i.e., the overall size of the swollen or coiled polymer molecule) and the frictional forces between polymer segments and the surrounding solvent.[35] For the solutions investigated here, the terpolymer concentrations are well above the expected critical micelle concentration (CMC; *e.g.*, 0.13 to 0.5 wt.% for 59 kg mol^{-1} ISD from Ref. 7) so the displaced volume of individual terpolymer micelles and the micelle-solvent interactions are most important to consider.

Previous research by Radjabian, *et al.*[32] quantified the flow response of a particular SNIPS diblock copolymer solution (polystyrene-*b*-poly(4-vinylpyridine) in a solvent mixture of DMF/THF) and observed that the viscosity displayed a power-law, shear thinning response with exponents of approximately -1/2. It is possible that the higher polymer concentrations studied by Radjabian, *et al.*[32] (25 wt.% to 28 wt.%) form structures that would dissociate as shear rate is increased and cause the observed shear thinning response. In another previous study, Dorin, *et al.* [2] employed small angle x-ray scattering to characterize 59 kg mol^{-1} ISV triblock terpolymer solutions (in a solvent mixture of 7:3 DOX/THF). For the ISV solutions, only broad correlation peaks were observed for low concentration solutions (10-14 wt.% ISV) while the data displayed peaks consistent with micelles in a body centered cubic (BCC) lattice structure at concentrations of 16 wt.% ISV, which ultimately resulted in cast membrane active layers with pores displaying a simple cubic structure. Gu, *et al.* [14] conducted *in situ* grazing incidence small-angle x-ray scattering experiments on blade cast films of an identical ISV system to what is investigated here (43 kg mol^{-1}; solvent mixture of 7:3 DOX/THF). The 16 wt.% ISV solution was observed to be disordered at early times (after 4 s of evaporation) but after additional evaporation ($t > 16$ s), evidence of micelles in a BCC lattice structure was observed ($t = 16$ s) which eventually transitioned to simple cubic (SC) at longer times ($t > 40$ s).

In the present study, solution concentrations of 9, 12, and 15 wt.% were investigated in an evaporation-controlled rheometer cell; thus, compared to the previous studies outlined above, the solutions investigated here were more dilute and while terpolymer micelles are expected to form, the structure is likely to be disordered, causing the Newtonian behavior that was observed over the full range of shear rates (1-1000 s^{-1}). If robust micellar structures with long-range order were present in the solutions, a shear thinning response would be expected in Figure 3b, as the increased flow would disrupt the structures and result in a corresponding decrease in measured stress (and thus viscosity).

Because the molar mass of the three triblock terpolymers in solution are similar (see Table 1), the hierarchical behavior of Newtonian viscosities reported in Figure 3b are most likely due to differences in micelle size driven by variation in the C-block chemistry (in terms of the Hansen solubility parameter, δ) as well as the differences in block fraction (vol.%) and specifically the fraction of polystyrene in the molecule. Unfortunately, the three triblock terpolymers investigated here contain different C-block chemistries as well as different fractions of polystyrene; thus, it is not possible to fully deconvolute the separate impact of block chemistry and block fraction on the viscosities reported in Figure 3b. However, an attempt is made in the following paragraphs to provide some insight on the polymer conformation in solution, potential micelle structure, and ultimately the flow behavior of the solutions in this dilute, amorphous regime.

Table 2. Hansen solubility parameters for each component of the triblock terpolymer solutions.

Chemistry	**Solubility parameter δ (MPa$^{0.5}$)**
Polyisoprene [I]	17.4 [36]
Polystyrene [S]	19.1 [36]
Poly(4-vinylpyridine) [V]	23.0 [37]
Poly(*tert*-butyl methacrylate) [B]	18.0 [36]
Poly(*N*,*N*-dimethylacrylamide) [D]	19.9 [38]
Tetrahydrofuran [THF]	19.4 [36]
1,4-dioxane [DOX]	20.5 [39]

Table 2 reports the Hansen solubility parameter for each component of the terpolymer solutions. Because the A- and B-block of the ISV, ISB, and ISD molecules are the same, these blocks will most likely interact similarly with the surrounding solvent molecules and allow us to concentrate our analysis on the interaction of the C-block of each terpolymer molecule with the solvents (30% THF – 70% DOX). The C-blocks of ISB and ISD are likely to adopt an expanded or swollen conformation in solution because their solubility parameters are similar to those of the solvents. Conversely, the C-block of ISV may form a more coiled or collapsed conformation in the presence of the solvents due to greater differences in solubility parameters.[40] A more coiled molecule (or smaller micelle) would have reduced hydrodynamic drag compared with a swollen molecule, leading to a reduction in solution viscosity; thus, if solvent/C-block interactions are dominant, ISV would be expected to display the lowest viscosity. However, this trend is the opposite of what is observed in Figure 3b, where ISV has the greatest viscosity, implying that the viscosity response is impacted by more than just block-solvent interactions.

Besides the interaction between solvents and each individual C-block, there is also a possibility of interactions between the A-, B-, and C-blocks. In the case of ISB and ISD, the solubility parameters are fairly similar for all the blocks, ranging from 17.4 to 19.9 (see Table 2). However, for ISV the solubility parameter of the C-block is much larger (V: 23.0) than the A-block (S: 17.4) and B-block (I: 19.1); thus, this molecule is more likely to form an expanded conformation (and proportionately larger micelle) compared to ISB and ISD, which would increase the viscosity of

the solution. [33] [34] [35] Thus, if intramolecular interactions are dominant, ISV would be expected to display the highest viscosity, consistent with results displayed in Figure 3b.

Unfortunately, considering the block-solvent and block-block interactions does not conclusively explain the viscosity values displayed in Figure 3b; perhaps it is also important to consider the volume fraction of polystyrene (B-block) in the molecules. A greater concentration of polystyrene in the ISV (55 vol.%) compared to the ISB (41 vol.%) and ISD (43 vol.%) molecules is consistent with the increased viscosity of ISV solutions. Rangou, *et al.*[15] found a positive relationship between the viscosity of SNIPS polymer solutions and the concentration of polystyrene in the polymer molecule as reduced viscosities were measured for polystyrene-*b*-poly(4-vinylpyridine) diblock copolymer solutions with increasing 4-vinylpyridine fraction (and proportionally less polystyrene). The authors do not attempt to explain this behavior; however, it is likely that the relatively large ("bulky") phenyl group of the styrene segments results in steric hindrance that manifests as an overall increase in molecule volume and thus greater hydrodynamic drag in solution. [41] Consequently, in the present investigation, the greater concentration of polystyrene in ISV may increase the molecule (micelle) volume compared with ISD and ISB and result in increased viscosity of the solution, again consistent with the results displayed in Figure 3b.

In summary, the hierarchical viscosity behavior of 15 wt.% ISV, ISB, and ISD triblock terpolymer solutions may be the result of the relative magnitudes of hydrodynamic drag forces caused by the different conformations adopted by the triblock terpolymers in solution which are believed to result in the formation of larger, disordered micelles within ISV solutions compared with ISD and ISB solutions. The observations in Figure 3b are most likely controlled by a combination of the factors described above; e.g., viscosity increases could be the combined result of the dominance of block-block interactions over block-solvent interactions and the steric hindrance contributions of polystyrene.

4.2 Viscoelastic behavior with significant evaporation

In a block polymer solution with minimal solvent evaporation (see Figure 3a), the enthalpic intermolecular interactions of the block polymer are partially screened by the solvent molecules, [35] and the viscosity of the solution does not depend on mobility of the individual polymer segments.[42] However, in the absence of solvent, polymer-to-polymer intermolecular interactions increase due to the enthalpic interaction of each segment of the block polymer,[20] and significant solvent evaporation drives the system to form nanodomains in solution.[32] Pendergast, *et al.*[43] have previously speculated that for a triblock terpolymer solution undergoing SNIPS, the resulting selective layer upon solvent evaporation is composed of a polystyrene matrix with spherical inclusions of polyisoprene and a cubic network of channels of the respective third block. The evaporation of the solvent is the initial step towards the creation of a viscoelastic film containing these phase-segregated pores.

In the triblock terpolymer solutions studied here, the development of the mechanical strength with time in Figure 5 is attributed to the formation of a viscoelastic film at the edge of the parallel plates

(illustrated in Figure 9). The viscoelastic film can be thought of as a "skin" and is typically found in asymmetric membranes obtained from precipitation of polymer solutions.[30] Figure 9 shows the hypothesized location of a viscoelastic film that is formed as a result of the progressive removal of solvent. Film formation initiates at the air-liquid interface and grows radially toward the center of the parallel plates, acting as a physical barrier that delays the migration of solvent from the bulk to the air-liquid interface.[30] The *G'* and *G"* response, the cross-over point, and the *G'* plateau behavior is mainly attributed to the mechanical strength development of this viscoelastic film which, in turn, depends on the chemistry of the polymer molecules and the initial polymer concentration in the solutions.

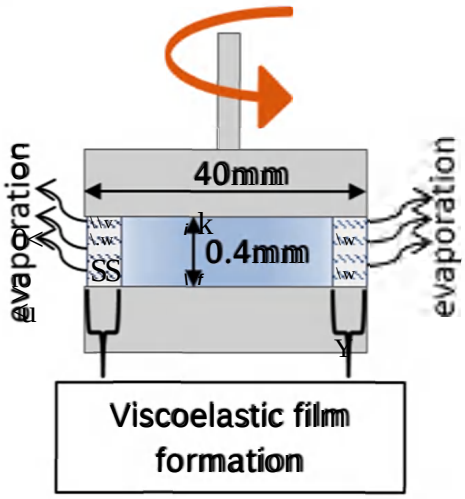

Figure 9. Hypothesized location of an evaporation-induced viscoelastic film formed during oscillatory testing in a 40 mm parallel plate fixture.

The differences in mechanical strength development reported in Figure 5 at the same polymer concentration may be attributed to the possible long-range lattice organization based on the differences in block chemistry of each sample. Sargent, *et al.* [7] previously reported that ISD terpolymer solutions (59 kg mol^{-1}) formed individual micelles at low polymer concentrations (<1 wt.%) and long-range lattices at significantly higher polymer concentration (>22 wt.%) using DOX as solvent. Dorin, *et al.* [2] showed that 16 wt.% ISV terpolymer solutions (59 kg mol^{-1}) organized into lattices using a 7:3 THF:DOX solvent mixture. Meanwhile Gu, *et al.* [14] showed that the type and extent of micellar organization within ISV terpolymer solutions (43 kg mol^{-1}) was a function of solvent concentration.

All three studies mentioned above convey the idea that the long-range micelle organization is directly connected to the final pore structure of the selective layer of SNIPS membranes. Then, the type and extent of the mechanical response to deformation depends on the type of lattice structure and the evolution of the lattice structure over time. Unfortunately, due to difference between each study and the samples used in the present experiments, there is insufficient evidence to accurately correlate the effect of micellar organization on the mechanical strength development reported in Figure 5 and the trend differences of data reported in Figure 6a. However, in all cases, micelle

assembly and long-range ordering as well as the bulk mechanical response to deformation also depends on the mobility of the individual polymer molecules. Consequently, here an attempt is made to better understand the mechanical responses reported in Figure 5 from the perspective of individual molecules. Upon solvent evaporation, the intermolecular distance between polymer chains (and micelles) is greatly reduced and the surface area of polymer chains in contact with each other increases, which in turn, increases the energy required for polymer chains to translate past each other. [44] The increase in energy required for motion, including local conformation changes, is intensified if the polymer molecule has relatively bulky side groups attached to the backbone.[44] [45] Consequently, a greater amount of energy, proportional to the concentration and type of side group, must be applied to induce molecular motion and, specifically, the deformation and restructuring of micelles. [41] [46]

In this work, all three terpolymer molecules contain bulky side groups within the B- and C-block. The B-block is a relatively stiff macromolecule (polystyrene) with large phenyl rings as side groups. The C-block contains 4-vinylpyridine in ISV, *tert*-butyl methacrylate in ISB, and *N*,*N*-dimethylacrylamide in ISD (see Figure 1). As shown in Figure 5, the growth rate of *G'* and *G"* is dependent on polymer chemistry and polymer initial concentration. These trends may be partly explained by considering the rotational barrier energies of chemical structures that are analogous to the bulky side groups of the ISV, ISB, and ISD. Bryantsev, *et al.*[47] reported rotational barrier energy values for alkyl- and phenyl-substituted urea around a C-N bond: 0.86-2 kcal/mol for methylurea, 5.2-9 kcal/mol for tert-butylurea, and 9-15 kcal/mol phenylurea. Due to the similarities in chemical structure, the methylurea groups that Bryantsev, *et al.* studied are a close representation of the *N*,*N*-dimethylacrylamide groups in the ISD molecule. In the same way, tert-butylurea is representative of *tert*-butyl methacrylate in ISB, and, phenylurea is analogous to phenyl rings (B-block) and 4-vinylpyridine in ISV. Then, considering the rotational barrier values reported by Bryantsev *et al.* for each bulky side group in the C-block, it is expected that 4-vinylpyridine will restrict the ability of ISV molecules (and micelles) to translate past each other to a greater extent than the *tert*-butyl methacrylate and *N*,*N*-dimethylacrylamide groups in ISB and ISD, respectively.[41] [45] In addition, the greater concentration of polystyrene that ISV contains over ISB and ISD (see vol.% in Table 1) represents a higher density of bulky side groups per molecule with the highest rotational barrier. Subsequently, ISV molecules (and micelles) are expected to require greater input energy compared to ISB and ISD molecules to deform a given amount,[41] consistent with the results in Figure 5 and the trends displayed by ISV solutions in Figure 6a (greatest initial slopes) and Figure 6c (greatest average *G'* plateau.)

Initial polymer concentration has a strong influence on the temporal cross-over points reported in Figure 7. In general, the viscous-to-elastic transition occurs at reduced times for solutions with greater initial polymer concentrations (and thus greater solution viscosity). If the solvent diffusion coefficient is considered the same for all samples (as was found here), then the viscous-to-elastic transition is also dependent on the type and density of bulky side groups present in the molecule. ISD solutions displayed the greatest transition times for all initial polymer concentrations (9 wt.%:

208 s; 12 wt.%: 84 s; 15 wt.%: 34 s). The viscous-to-elastic transition for 9 wt.% ISV and ISB solutions occurred more quickly (32 s, 96 s, respectively); and the cross-over points for 12 wt.% and 15 wt.% ISV and ISB solutions are not shown in Figure 7 because the viscous-to-elastic transition apparently happens very fast ($t < 4$ s, beyond the measurement window of the experiment). These results are consistent to the analysis of rotational barriers for ISV, ISB and ISD molecules.

In summary, the observed order of the oscillatory rheometry results agrees well with the rotational rheometry results. ISV solutions displayed the greatest initial viscosity as well as the fastest development and greatest magnitude of mechanical strength. The viscosity behavior of each solution is attributed to the dominant block-block interactions and the steric hindrance of polystyrene which most likely manifests in the formation of larger micelles in the ISV solutions compared with ISB and ISD solutions. Upon solvent evaporation, mechanical strength develops as the terpolymer micelles order into lattices, the initial rate of which may be controlled by the presence of bulky side groups in the C-blocks of each molecule and their different rotational barriers. As solvent evaporation proceeds further, additional restructuring is possible. For example, in addition to segregation of poly(4-vinylpyridine) from polystryrene and polyisoprene in ISV, the polyisoprene blocks segregate from the polystryrene blocks which is most likely responsible for the observed transition from BCC to SC observed by Gu, *et al*. [14] for 16 wt.% ISV solutions. There then will exist domains of poly(4-vinylpyridine) and polyisoprene in a matrix of polystryrene, and the observed resistance to shear is likely dependent on the energy required to deform the ordered lattice and its rate of evolution (e.g., from BCC to SC) than on the rotational barrier energies of the molecular structures of individual molecules.

4.3 The block chemistry effect over the solvent evaporation rate

The similar diffusion coeficient (D) of a THF-DOX solvent mixture in ISV, ISB, and ISD films is attributed to the similar chemical structure of the triblock terpolymer molecules and, specifically, the isoprene-styrene matrix that forms upon solvent evaporation. On average, 75% of the triblock terpolymer molecules are composed of polyisoprene and polystyrene blocks in relatively similar proportions. Having a very similar matrix to diffuse through, it is not surprising that the rate of solvent diffusion is in fact very similar for the different films.[48]

5.0 SUMMARY AND CONCLUSIONS

The role of the triblock terpolymer chemistry and solvent evaporation over the mechanical strength development of polymer solutions used to fabricate membranes via SNIPS process was studied. Three different polymer chemistries with similar molar mass were analyzed. Shear rheometry was used to quantify the flow behavior under minimal and significant solvent evaporation conditions. The solvent diffusion coefficients through different polymer films were also measured and found to be independent of initial solution concentration (9 wt.%, 12 wt.%, and 15 wt.% polymer in solution) and triblock terpolymer composition (ISV, ISB, and ISD). Results suggested that:

- For all triblock terpolymer solutions investigated here, solvent evaporation resulted in the formation of a viscoelastic film typical of asymmetric membranes. The development rate and magnitude of the film's mechanical strength was successfully measured with oscillatory rheometry and parallel-plate fixtures.
- For all triblock terpolymer compositions, increased initial concentration of terpolymer in solution resulted in greater solution viscosities (found to be Newtonian), faster strength development, and greater strength magnitudes.
- Solution properties – viscosity and mechanical strength development – were strongly dependent on the chemical structure of the triblock terpolymer molecules. A hierarchical order (ISV>ISB>ISD) in magnitude was observed for both properties, with ISV solutions displaying the greatest solution viscosity and fastest strength development and greatest strength magnitude of the evaporation-induced viscoelastic film.
- Block-block and block-solvent interactions as well as the concentration of polystyrene within the terpolymer molecules are believed to be the factors that most influenced the experimental results by directly impacting the relative size of terpolymer micelles that are expected to form in solution and the ability of the micelles to order and restructure as solvent evaporates.

The findings above may have a potential use to tailor the final microstructure of SNIPS filtration membranes. The viscosity of polymer solutions can be tailored based on the physical and chemical information of the selected polymer molecule. In this specific case, it can be speculated that ISV polymer solutions will require a smaller concentration of polymer than ISB and ISD solutions to achieve a desired viscosity, micelle mobility, and a final macro-void support layer.

ACKNOWLEDGEMENTS

This research is based upon work supported by the National Science Foundation under Grant No. 1436255 (K.A.E, B.W.B., W.A.P.) and DMR-1707836 (U.B.W.).

6.0 REFERENCES

(1) Peinemann, K.-V.; Abetz, V.; Simon, P. F. W. **2007**.

(2) Dorin, R. M.; Marques, D. S.; Sai, H.; Vainio, U.; Phillip, W. a; Peinemann, K.-V.; Nunes, S. P.; Wiesner, U. *ACS Macro Lett.* **2012**, *1* (5), 614–617.

(3) Mulvenna, R. a.; Weidman, J. L.; Jing, B.; Pople, J. a.; Zhu, Y.; Boudouris, B. W.; Phillip, W. a. *J. Memb. Sci.* **2014**, *470*, 246–256.

(4) Y. Zhang, J. L. Sargent, B. W. Boudouris, W. A. P. *J. Appl. Polym. Sci.* **2015**, *41683*, 17.

(5) Weidman, J. L.; Mulvenna, R. A.; Boudouris, B. W.; Phillip, W. A. *Langmuir* **2015**, *31* (40), 11113–11123.

(6) Dorin, R. M.; Phillip, W. a.; Sai, H.; Werner, J.; Elimelech, M.; Wiesner, U. *Polym. (United Kingdom)* **2014**, *55* (1), 347–353.

(7) Sargent, J. L.; Hoss, D. J.; Phillip, W. A.; Boudouris, B. W. *J. Appl. Polym. Sci.* **2017**, *45531*, 1–8.

(8) Poole, J. L.; Donahue, S.; Wilson, D.; Li, Y. M.; Zhang, Q.; Gu, Y.; Ferebee, R.; Lu, Z.; Dorin, R. M.; Hancock, L. F.; Takiff, L.; Hakem, I. F.; Bockstaller, M. R.; Wiesner, U.; Walker, J. *Macromol. Rapid Commun.* **2017**, *1700364*, 1700364.

(9) Yang, S. Y.; Park, J.; Yoon, J.; Ree, M.; Jang, S. K.; Kim, J. K. *Adv. Funct. Mater.* **2008**, *18* (9), 1371–1377.

(10) Gu, Y.; Werner, J. G.; Dorin, R. M.; Robbins, S. W.; Wiesner, U. *Nanoscale* **2015**, *7* (13), 5826–5834.

(11) Weidman, J. L.; Mulvenna, R. A.; Boudouris, B. W.; Phillip, W. A. *J. Am. Chem. Soc.* **2016**, *138* (22), 7030–7039.

(12) Dorin, R. M.; Sai, H.; Wiesner, U. *Chem. Mater.* **2014**, *26* (1), 339–347.

(13) U.S. Department of Energy. In *Innovating clean energy technologies in advance manufacturing*; 2015, Q. T. R., Ed.; 2015; p 34.

(14) Gu, Y.; Dorin, R. M.; Tan, K. W.; Smilgies, D. M.; Wiesner, U. *Macromolecules* **2016**, *49* (11), 4195–4201.

(15) Rangou, S.; Buhr, K.; Filiz, V.; Clodt, J. I.; Lademann, B.; Hahn, J.; Jung, A.; Abetz, V. *J. Memb. Sci.* **2014**, *451*, 266–275.

(16) Li, Y. M.; Zhang, Q.; Álvarez-Palacio, J. R.; Hakem, I. F.; Gu, Y.; Bockstaller, M. R.; Wiesner, U. *Polym. (United Kingdom)* **2017**, *126*, 368–375.

(17) Phillip, W. a; Dorin, R. M.; Werner, J.; Hoek, E. M. V; Wiesner, U.; Elimelech, M. *Nano Lett.* **2011**, *11* (7), 2892–2900.

(18) Phillip, W. a.; Hillmyer, M. a.; Cussler, E. L. *Macromolecules* **2010**, *43* (18), 7763–7770.

(19) Schaefer, C.; Van Der Schoot, P.; Michels, J. J. *Phys. Rev. E - Stat. Nonlinear, Soft Matter Phys.* **2015**, *91* (2), 1–6.

(20) Arya, R. K. *J. Chem. Eng.* **2012**, *C* (1), 12–20.

(21) Macosko, C. W. *Rheology: Principles, measurements, and applications*; Wiley-Blackwell, 1995; Vol. 41.

(22) Chassenieux, C.; Nicolai, T.; Benyahia, L. *Curr. Opin. Colloid Interface Sci.* **2011**, *16* (1), 18–26.

(23) Winnik, M. A.; Yekta, A. *Curr. Opin. Colloid Interface Sci.* **1997**, *2* (4), 424–436.

(24) Hamley, I. W. *Block copolymers in solution : fundamentals and applications*; Wiley, 2005.

(25) Zhou, J.; Man, X.; Jiang, Y.; Doi, M. *Adv. Mater.* **2017**, *29* (45), 1703769.

(26) Moad, G.; Rizzardo, E.; Thang, S. H. *Living radical polymerization by the RAFT process*;

2005; Vol. 58.

(27) Crank, J. *The Mathematics of Diffusion*, 2nd ed.; Oxford University Press, 1975.

(28) Bird, R. B.; Stewart, W. E.; Lightfoot, E. N. *Transport phenomena*; J. Wiley, 2007.

(29) Atkinson, P. M.; Lloyd, D. R. *J. Memb. Sci.* **2000**, *171* (1), 1–18.

(30) Strathmann, H.; Kock, K. *Desalination* **1977**, *21* (3), 241–255.

(31) Zhang, Q.; Li, Y. M.; Gu, Y.; Dorin, R. M.; Wiesner, U. *Polym. (United Kingdom)* **2016**, *107*, 398–405.

(32) Radjabian, M.; Koll, J.; Buhr, K.; Vainio, U.; Abetz, C.; Handge, U. a.; Abetz, V. *Polymer (Guildf).* **2014**, *55* (13), 2986–2997.

(33) Brust, M.; Schaefer, C.; Doerr, R.; Pan, L.; Garcia, M.; Arratia, P. E.; Wagner, C. *Phys. Rev. Lett.* **2013**, *110* (7), 6–10.

(34) Cassagnau, P. *Polym. (United Kingdom)* **2013**, *54* (18), 4762–4775.

(35) Larson, R. G. *The structure and rheology of complex fluids*; Oxford University Press, 2005.

(36) H. G. Barth, R. E. M. *LCGC North Am.* **2013**, *31* (1), 14–29.

(37) O'Driscoll, S.; Demirel, G.; Farrell, R. A.; Fitzgerald, T. G.; O'Mahony, C.; Holmes, J. D.; Morris, M. A. *Polym. Adv. Technol.* **2011**, *22* (6), 915–923.

(38) Krevelen, D. W. van (Dirk W.; Nijenhuis, K. te. *Properties of polymers : their correlation with chemical structure ; their numerical estimation and prediction from additive group contributions*; Elsevier, 2009.

(39) Hansen, C. M. *Hansen solubility parameters : a user's handbook*; CRC Press, 2007.

(40) Pendergast, M. M.; Mika Dorin, R.; Phillip, W. A.; Wiesner, U.; Hoek, E. M. V. *J. Memb. Sci.* **2013**, *444*, 461–468.

(41) Bueche, F. *J. Chem. Phys.* **1953**, *21* (10), 1850.

(42) Adam, M.; Delsanti, M. *J. Phys.* **1982**, *43* (3), 549–557.

(43) Pendergast, M. M.; Mika Dorin, R.; Phillip, W. a.; Wiesner, U.; Hoek, E. M. V. *J. Memb. Sci.* **2013**, *444*, 461–468.

(44) Brueggeman, B. G.; Minnick, M. G.; Schrag, J. L. *Macromolecules* **1978**, *11* (1), 119–126.

(45) Shaw, M. T.; MacKnight, W. J. *Introduction to Polymer Viscoelasticity*, 3rd ed.; John Wiley & Sons, Inc., 2005.

(46) Lenhart, J. L.; Fischer, D. A.; Chantawansri, T. L.; Andzelm, J. W. *Langmuir* **2012**, *28* (44), 15713–15724.

(47) Bryantsev, V. S.; Firman, T. K.; Hay, B. P. *J. Phys. Chem.* **2005**, *109* (5), 832–842.

(48) Tsige, M.; Grest, G. S. *J. Phys. Condens. Matter* **2005**, *17* (49), S4119–S4132.